Technical Report: Sparse Doubly-Selective Channel Estimation Techniques for OSTBC MIMO-OFDM Systems: A Hierarchical Bayesian Kalman Filter Based Approach

Suraj Srivastava, Amrita Mishra, Aditya K. Jagannatham and Lajos Hanzo

I. Complexity Analysis

The per EM complexity for each block of the proposed P-HBKF and D-HBKF schemes are determined as follows. Table I presents the complexities of the various steps in the P-HBKF scheme for estimation of the sparse channel $\mathbf{h}_n$ using the Algorithm 1 described in the manuscript. The complexities of the various intermediate steps in the joint estimation of the sparse channel $\mathbf{h}_n$ and data detection $\widehat{\mathbf{a}}^{(i)}_{k,n}(m)$ in the D-HBKF technique are similarly given in Table II. The dominant terms in each Table are presented in red color.

TABLE I: Computational Complexity of P-HBKF Technique

Steps in P-HBKF	Multiplications	Additions
Computation of $\widehat{\mathbf{y}}_{\mathcal{P},n\|n-1}$ using Eq.(73)	$LN_RN_T + N_PN_cN_R^3L^2N_T^2$	$N_PN_cN_R^3L^2N_T^2 - N_PN_cN_R^2LN_T$
Computation of $\mathbf{y}_{\mathcal{P},e,n}$ using Eq.(76)	$-$	$N_PN_cN_R$
Computation of $\mathbf{\Sigma}_n^{(i)}$ in E-Step	$L^2N_R^3N_T^2N_PN_c + \frac{1}{2}L^3N_R^3N_T^3$ $+\frac{3}{2}L^2N_R^2N_T^2 + LN_RN_T$	$L^2N_R^3N_T^2N_PN_c + \frac{1}{2}L^3N_R^3N_T^3$ $-\frac{3}{2}L^2N_R^2N_T^2 + LN_RN_T$
Computation of $\boldsymbol{\mu}_n^{(i)}$ in E-Step	$L^2N_R^3N_T^2N_PN_c + LN_R^2N_TN_PN_c$	$L^2N_R^3N_T^2N_PN_c - LN_RN_T$
Computation of $\widehat{\mathbf{\Gamma}}_n^{(i)}$ in M-Step	$LN_RN_T + 2L$	$2LN_RN_T - 2L$
Computation of $\mathbf{M}_{n\|n-1}$ using Eq.(74)	$L^2N_R^2N_T^2 + LN_RN_T$	LN_RN_T
Computation of $\mathbf{K}_n$ using Eq.(75)	$2N_PN_cN_R^3L^2N_T^2 + 2N_P^2N_c^2N_R^3LN_T$	$2N_PN_cN_R^3L^2N_T^2 - 2N_PN_cN_R^2LN_T$ $2N_P^2N_c^2N_R^3LN_T - LN_TN_PN_cN_R^2$ $N_PN_cN_R - N_P^2N_c^2N_R^2$
Computation of $\widehat{\mathbf{h}}_{n\|n}$ using Eq.(77)	$LN_R^2N_TN_PN_c$	$LN_R^2N_TN_PN_c$
Computation of $\mathbf{M}_{n\|n}$ using Eq.(78)	$L^2N_R^3N_T^2N_PN_c + L^3N_R^3N_T^3$	$L^2N_R^3N_T^2N_PN_c + L^3N_R^3N_T^3$ $LN_RN_T - 2L^2N_R^2N_T^2$

TABLE II: Computational Complexity of D-HBKF Technique

Steps in D-HBKF	Multiplications	Additions
Computation of $\widehat{\mathbf{y}}_{\mathcal{B},n\|n-1}$ using Eq.(73)	$LN_RN_T + KNN_cN_R^3L^2N_T^2$	$KNN_cN_R^3L^2N_T^2 - KNN_cN_R^2LN_T$
Computation of $\mathbf{y}_{\mathcal{B},e,n}$ using Eq.(76)	$-$	KNN_cN_R
Computation of $\mathbf{\Sigma}_{\mathcal{B},n}^{(i)}$ in E-Step	$L^2N_R^3N_T^2KNN_c + \frac{1}{2}L^3N_R^3N_T^3 + \frac{3}{2}L^2N_R^2N_T^2 + LN_RN_T$	$L^2N_R^3N_T^2KNN_c + \frac{1}{2}L^3N_R^3N_T^3 - \frac{3}{2}L^2N_R^2N_T^2 + LN_RN_T$
Computation of $\boldsymbol{\mu}_{\mathcal{B},n}^{(i)}$ in E-Step	$L^2N_R^3N_T^2KNN_c + LN_R^2N_TKNN_c$	$L^2N_R^3N_T^2KNN_c - LN_RN_T$
Computation of $\widehat{\mathbf{\Gamma}}_n^{(i)}$ in M-Step	$LN_RN_T + 2L$	$2LN_RN_T - 2L$
Computation of $\mathbf{M}_{n\|n-1}^{(i)}$ using Eq.(74)	$L^2N_R^2N_T^2 + LN_RN_T$	LN_RN_T
Computation of $\mathbf{K}_n^{(i)}$ using Eq.(75)	$2KNN_cN_R^3L^2N_T^2 + 2K^2N^2N_c^2N_R^3LN_T$	$2KNN_cN_R^3L^2N_T^2 - 2KNN_cN_R^2LN_T$ $2K^2N^2N_c^2N_R^3LN_T - LN_TKNN_cN_R^2$ $KNN_cN_R - K^2N^2N_c^2N_R^2$
Computation of $\widehat{\mathbf{h}}_{n\|n}^{(i)}$ using Eq.(77)	$LN_R^2N_TKNN_c$	$LN_R^2N_TKNN_c$
Computation of $\mathbf{M}_{n\|n}^{(i)}$ using Eq.(78)	$L^2N_R^3N_T^2KNN_c + L^3N_R^3N_T^3$	$L^2N_R^3N_T^2KNN_c + L^3N_R^3N_T^3$ $LN_RN_T - 2L^2N_R^2N_T^2$
Computation of $\widehat{\boldsymbol{\mathcal{H}}}_n^{(i)}$ using Eq.(64)	NN_RN_TL	$NN_TN_R(L-1)$
Computation of $\widetilde{\mathbf{M}}_n^{(i)}$ in Eq.(72)	$N_T^3N_R^3NL^2 + N_T^3N_R^3N^2L$	$N_R^3N_T^3L^2N + N_T^3N_R^3N^2L$ $-N_R^2N_T^2LN - N_R^2N_T^2N^2$
Computation of $\zeta_n^{(i)}(m)$ using Eq.(72)	N_TN_RN	$2N_TN_RN - 2N$
Computation of $\boldsymbol{\mathcal{C}}_n(m)$ using Eq.(65)	$2N_RN_TN_cN_sN$	$2N_RN_TN_cN_sN + 2N_RN_cN_sN$
Computation of $\widehat{\mathbf{a}}_{k,n}^{(i)}(m)$ using Eq.(71)	$2N_sN_RN_cKN + 2N_sKN$	$2N_sN_RN_cKN - 2N_sKN$

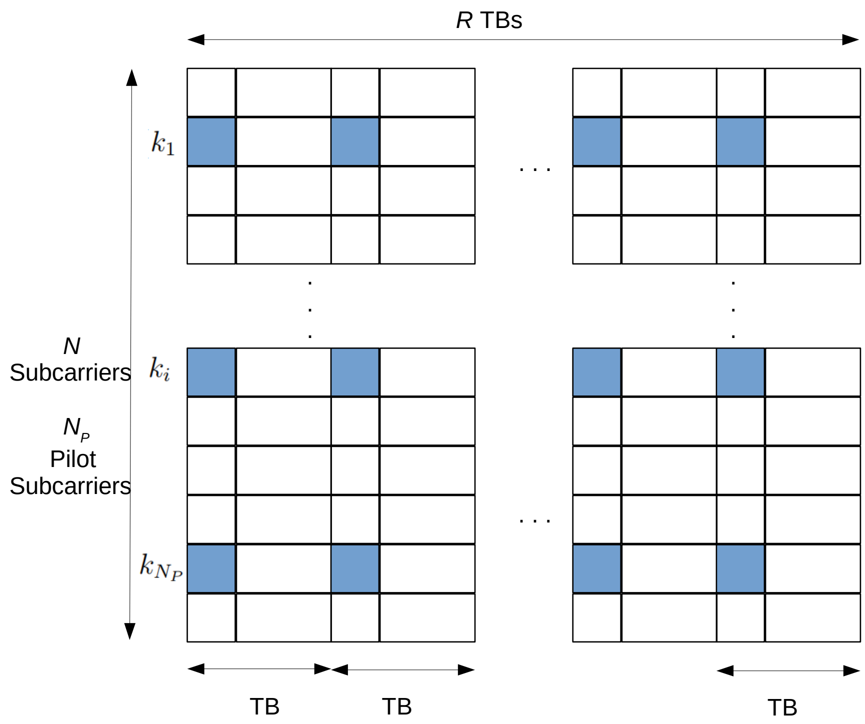

Fig. 1: Pilot pattern for the proposed OSTBC MIMO-OFDM systems

II. Derivation of 2D-MMSE

Let us consider the pilot pattern of the proposed OSTBC MIMO-OFDM system, as shown in Figure 1. The pilot matrix $\mathbf{Y}_n(m) \in \mathbb{C}^{N_R \times N_c}$ received in the nth transmission block (TB) and the mth subcarrier is given by

$$\mathbf{Y}_n(m) = \mathbf{H}_n(m)\mathbf{X}_n(m) + \mathbf{W}_n(m), \tag{1}$$

where $\mathbf{H}_n(m) \in \mathbb{C}^{N_R \times N_T}$ and $\mathbf{X}_n(m) \in \mathbb{C}^{N_T \times N_c}$ denote the MIMO CFR and the OSTBC pilot codeword, respectively, and $\mathbf{W}_n(m) \in \mathbb{C}^{N_R \times N_c}$ denotes the AWGN matrix. Note that an OSTBC pilot codeword $\mathbf{X}_n(m)$ is comprised of N_c time slots. The vectorized system model corresponding to (1) is obtained as

$$\begin{aligned} \mathbf{y}_n(m) &= \mathrm{vec}(\mathbf{Y}_n(m)) \\ &= \underbrace{\left(\mathbf{X}_n^T(m) \otimes \mathbf{I}_{N_R}\right)}_{\mathbf{\Phi}_n(m) \in \mathbb{C}^{(N_R N_c) \times (N_R N_T)}} \mathbf{h}_n(m) + \mathbf{w}_n(m), \end{aligned} \tag{2}$$

where $\mathbf{h}_n(m) = \text{vec}[\mathbf{H}_n(m)] \in \mathbb{C}^{(N_R N_T)\times 1}$ denotes the vectorized CFR and $\mathbf{w}_n(m) = \text{vec}[\mathbf{W}_n(m)]$. Let $\{k_1, k_2, \ldots, k_{N_P}\}$ denote the set of indices of the pilot subcarriers. The channel estimation model for the nth TB is obtained by stacking all the pilot outputs as

$$\underbrace{\begin{bmatrix} \mathbf{y}_n(k_1) \\ \mathbf{y}_n(k_2) \\ \vdots \\ \mathbf{y}_n(k_{N_P}) \end{bmatrix}}_{\mathbf{y}_n \in \mathbb{C}^{(N_R N_c N_P)\times 1}} = \underbrace{\begin{bmatrix} \mathbf{\Phi}_n(k_1) & \mathbf{0} & \ldots & \mathbf{0} \\ \mathbf{0} & \mathbf{\Phi}_n(k_2) & \ldots & \mathbf{0} \\ \vdots & \vdots & & \vdots \\ \mathbf{0} & \mathbf{0} & \ldots & \mathbf{\Phi}_n(k_{N_P}) \end{bmatrix}}_{\mathbf{\Phi}_n} \underbrace{\begin{bmatrix} \mathbf{h}_n(k_1) \\ \mathbf{h}_n(k_2) \\ \vdots \\ \mathbf{h}_n(k_{N_P}) \end{bmatrix}}_{\mathbf{h}_n \in \mathbb{C}^{(N_R N_T N_P)\times 1}} + \underbrace{\begin{bmatrix} \mathbf{w}_n(k_1) \\ \mathbf{w}_n(k_2) \\ \vdots \\ \mathbf{w}_n(k_{N_P}) \end{bmatrix}}_{\mathbf{w}_n},$$

$$\Rightarrow \mathbf{y}_n = \mathbf{\Phi}_n \mathbf{h}_n + \mathbf{w}_n. \tag{3}$$

Furthermore, stacking $\mathbf{y}_n, \forall\ 1 \leq n \leq R$, the equivalent pilot-based channel estimation model corresponding to all the R TBs is obtained as

$$\underbrace{\begin{bmatrix} \mathbf{y}_1 \\ \mathbf{y}_2 \\ \vdots \\ \mathbf{y}_R \end{bmatrix}}_{\mathbf{y} \in \mathbb{C}^{(N_R N_c N_P R)\times 1}} = \underbrace{\begin{bmatrix} \mathbf{\Phi}_1 & \mathbf{0} & \ldots & \mathbf{0} \\ \mathbf{0} & \mathbf{\Phi}_2 & \ldots & \mathbf{0} \\ \vdots & \vdots & & \vdots \\ \mathbf{0} & \mathbf{0} & \ldots & \mathbf{\Phi}_R \end{bmatrix}}_{\mathbf{\Phi}} \underbrace{\begin{bmatrix} \mathbf{h}_1 \\ \mathbf{h}_2 \\ \vdots \\ \mathbf{h}_R \end{bmatrix}}_{\mathbf{h} \in \mathbb{C}^{(N_R N_T N_P R)\times 1}} + \underbrace{\begin{bmatrix} \mathbf{w}_1 \\ \mathbf{w}_2 \\ \vdots \\ \mathbf{w}_R \end{bmatrix}}_{\mathbf{w}},$$

$$\Rightarrow \mathbf{y} = \mathbf{\Phi} \mathbf{h} + \mathbf{w}. \tag{4}$$

Let the vectorized CFR $\tilde{\mathbf{h}}_n \in \mathbb{C}^{(N_R N_T N)\times 1}$ corresponding to the pilot and data subcarrier locations in the nth TB be defined as

$$\tilde{\mathbf{h}}_n = \left[\mathbf{h}_n^T(1), \mathbf{h}_n^T(2), \ldots, \mathbf{h}_n^T(N)\right]^T. \tag{5}$$

Similarly, the vectorized CFR $\tilde{\mathbf{h}} \in \mathbb{C}^{(N_R N_T N R)\times 1}$ corresponding to the pilot and data subcarrier locations for the entire estimation block can be defined as

$$\tilde{\mathbf{h}} = \left[\tilde{\mathbf{h}}_1^T, \tilde{\mathbf{h}}_2^T, \ldots, \tilde{\mathbf{h}}_R^T\right]^T. \tag{6}$$

The 2D-MMSE estimate of the overall CFR $\tilde{\mathbf{h}}$ is obtained as [1]

$$\hat{\tilde{\mathbf{h}}} = \mathbf{C}\mathbf{y}, \tag{7}$$

where $\mathbf{C} \in \mathbb{C}^{(N_R N_T N R)\times(N_R N_c N_P R)}$ denotes the linear estimation matrix. By exploiting the orthogonality principle, we have:

$$\mathbb{E}\left[\left(\hat{\tilde{\mathbf{h}}} - \tilde{\mathbf{h}}\right)\mathbf{y}^H\right] = \mathbb{E}\left[\left(\mathbf{C}\mathbf{y} - \tilde{\mathbf{h}}\right)\mathbf{y}^H\right] = \mathbf{0}, \tag{8}$$

which derives the estimation matrix $\mathbf{C}$ as

$$\mathbf{C} = \mathbf{R}_{\tilde{h}y}\mathbf{R}_{yy}^{-1}, \tag{9}$$

where $\mathbf{R}_{yy} = \mathbb{E}\left[\mathbf{y}\mathbf{y}^H\right] \in \mathbb{C}^{(N_R N_c N_P R)\times(N_R N_c N_P R)}$ denotes the auto-correlation matrix of the received pilot output $\mathbf{y}$ and $\mathbf{R}_{\tilde{h}y} = \mathbb{E}\left[\tilde{\mathbf{h}}\mathbf{y}^H\right] \in \mathbb{C}^{(N_R N_T N R)\times(N_R N_c N_P R)}$ represents the cross-correlation matrix of the CFR vector $\tilde{\mathbf{h}}$ and the received pilot output $\mathbf{y}$. Using the notations above, the 2D-MMSE estimate is derived as

$$\hat{\tilde{\mathbf{h}}} = \mathbf{R}_{\tilde{h}y}\mathbf{R}_{yy}^{-1}\mathbf{y}. \tag{10}$$

Assuming the samples of the noise vector $\mathbf{w}$ to be independent and identically distributed with power σ_w^2, the auto-correlation matrix $\mathbf{R}_{yy}$ can be further simplified to

$$\begin{aligned}\mathbf{R}_{yy} &= \mathbb{E}\left[\mathbf{y}\mathbf{y}^H\right]\\ &= \mathbf{\Phi}\mathbf{R}_{hh}\mathbf{\Phi}^H + \sigma_w^2\mathbf{I},\end{aligned} \tag{11}$$

where $\mathbf{R}_{hh} = \mathbb{E}\left[\mathbf{h}\mathbf{h}^H\right] \in \mathbb{C}^{(N_R N_T N_P R)\times(N_R N_T N_P R)}$ denotes the auto-correlation matrix of the CFR vector $\mathbf{h}$. Similarly, the cross-correlation matrix $\mathbf{R}_{\tilde{h}y}$ can be obtained as

$$\begin{aligned}\mathbf{R}_{\tilde{h}y} &= \mathbb{E}\left[\tilde{\mathbf{h}}\mathbf{y}^H\right]\\ &= \mathbf{R}_{\tilde{h}h}\mathbf{\Phi}^H,\end{aligned} \tag{12}$$

where the matrix $\mathbf{R}_{\tilde{h}h} = \mathbb{E}\left[\tilde{\mathbf{h}}\mathbf{h}^H\right] \in \mathbb{C}^{(N_R N_T N R)\times(N_R N_T N_P R)}$ denotes the crosscorrelation of the CFR vectors $\tilde{\mathbf{h}}$ and $\mathbf{h}$. The correlation matrix $\mathbf{R}_{hh}$ can be derived as follows.

The CFR vector $\mathbf{h}$ can be written in terms of its composite vectors $\mathbf{h}_n(k_i), 1 \leq n \leq R, 1 \leq i \leq N_P$, as

$$\mathbf{h} = \left[\mathbf{h}_1^T(k_1)\ldots\mathbf{h}_1^T(k_{N_P})\ \mathbf{h}_2^T(k_1)\ldots\mathbf{h}_2^T(k_{N_P})\ldots\ldots\mathbf{h}_R^T(k_1)\ldots\mathbf{h}_R^T(k_{N_P})\right]. \tag{13}$$

Thus, the auto-correlation matrix $\mathbf{R}_{hh} = \mathbb{E}\left[\mathbf{h}\mathbf{h}^H\right]$ can be computed from each component correlation matrix $\mathbf{R}_{h,n_1,k_i,n_2,k_j} \in \mathbb{C}^{(N_R N_T)\times(N_R N_T)}$ defined as

$$\mathbf{R}_{h,n_1,k_i,n_2,k_j} = \mathbb{E}\left[\mathbf{h}_{n_1}(k_i)\mathbf{h}_{n_2}^H(k_j)\right]. \tag{14}$$

Similarly, the quantity $\mathbf{R}_{h,n_1,k_i,n_2,k_j}$ can also be used to compute the crosscorrelation matrix $\mathbf{R}_{\tilde{h}h} = \mathbb{E}\left[\tilde{\mathbf{h}}\mathbf{h}^H\right]$. The matrix $\mathbf{R}_{h,n_1,k_i,n_2,k_j}$ is evaluated next using the power delay profile of the L-tap channel and the associated AR-1 model.

Let $\bar{\mathbf{H}}_{n_1}(l) \in \mathbb{C}^{N_R \times N_T}$ denote the time-domain lth MIMO channel tap in TB n_1. The associated CFR matrix $\mathbf{H}_{n_1}(k_i)$, which corresponds to the subcarrier index k_i in TB n_1, can be expressed as

$$\mathbf{H}_{n_1}(k_i) = \underbrace{\left[\bar{\mathbf{H}}_{n_1}(0)\ \bar{\mathbf{H}}_{n_1}(1)\ \ldots\ \bar{\mathbf{H}}_{n_1}(L-1)\right]}_{\bar{\mathbf{H}}_{n_1} \in \mathbb{C}^{N_R \times (LN_T)}} \left(\mathbf{f}_{k_i} \otimes \mathbf{I}_{N_T}\right), \tag{15}$$

where the truncated Fourier vector obeys $\mathbf{f}_{k_i} = \left[1, e^{-j\frac{2\pi k_i}{N}}, \ldots, e^{-j\frac{2\pi(L-1)k_i}{N}}\right]^T \in \mathbb{C}^{L\times 1}$. Defining the vectorized CIR as $\bar{\mathbf{h}}_{n_1} = \mathrm{vec}(\bar{\mathbf{H}}_{n_1}) \in \mathbb{C}^{(LN_RN_T)\times 1}$, the relationship between the vectorized CFR $\mathbf{h}_{n_1}(k_i)$ and $\bar{\mathbf{h}}_{n_1}$ can be obtained as

$$\begin{aligned}\mathbf{h}_{n_1}(k_i) &= \mathrm{vec}[\mathbf{H}_{n_1}(k_i)] \\ &= \mathbf{F}_{k_i}\bar{\mathbf{h}}_{n_1},\end{aligned} \tag{16}$$

where $\mathbf{F}_{k_i} = \left[\mathbf{f}_{k_i}^T \otimes \mathbf{I}_{N_RN_T}\right]$. Let $\bar{\mathbf{h}}_{n_1}(l) = \mathrm{vec}\left(\bar{\mathbf{H}}_{n_1}(l)\right)$ denote the vectorized lth tap and σ_l^2 denote the average power of each element of $\bar{\mathbf{h}}_{n_1}(l)$. This implies that $\mathbb{E}\left[\bar{\mathbf{h}}_{n_1}(l)\bar{\mathbf{h}}_{n_1}^H(l)\right] = \sigma_l^2\mathbf{I}_{N_RN_T}$. Furthermore, the auto-correlation of the vectorized CIR $\bar{\mathbf{h}}_{n_1} = \left[\bar{\mathbf{h}}_{n_1}^T(0), \bar{\mathbf{h}}_{n_1}^T(2), \ldots, \bar{\mathbf{h}}_{n_1}^T(L-1)\right]^T$, is derived as

$$\mathbb{E}\left[\bar{\mathbf{h}}_{n_1}\bar{\mathbf{h}}_{n_1}^H\right] = \begin{bmatrix} \sigma_1^2\mathbf{I}_{N_RN_T} & \mathbf{0} & \ldots & \mathbf{0} \\ \mathbf{0} & \sigma_2^2\mathbf{I}_{N_RN_T} & \ldots & \mathbf{0} \\ \vdots & \vdots & & \vdots \\ \mathbf{0} & \mathbf{0} & \ldots & \sigma_{L-1}^2\mathbf{I}_{N_RN_T} \end{bmatrix} = \left(\mathbf{P} \otimes \mathbf{I}_{N_RN_T}\right), \tag{17}$$

where the matrix $\mathbf{P} \in \mathbb{R}^{L\times L}$ is a diagonal matrix comprised of the average power $\{\sigma_l^2\}_{l=0}^{L-1}$ on its main diagonal. Furthermore, following the AR-1 model for the time-domain evolution of the channel, which is given as

$$\bar{\mathbf{h}}_n = \rho\bar{\mathbf{h}}_{n-1} + \sqrt{1-\rho^2}\bar{\mathbf{v}}_n, \tag{18}$$

one can also derive the cross-correlation $\mathbb{E}\left[\bar{\mathbf{h}}_{n_1}\bar{\mathbf{h}}_{n_2}^H\right]$ as

$$\mathbb{E}\left[\bar{\mathbf{h}}_{n_1}\bar{\mathbf{h}}_{n_2}^H\right] = \rho^{|n_1-n_2|}\left(\mathbf{P} \otimes \mathbf{I}_{N_RN_T}\right). \tag{19}$$

Using the results from (16) and (19), the cross-correlation matrix $\mathbf{R}_{h,n_1,k_i,n_2,k_j}$ of the vectorized CFRs $\mathbf{h}_{n_1}(k_i)$ and $\mathbf{h}_{n_2}(k_j)$, as defined in (14), can be derived as

$$\begin{aligned}\mathbf{R}_{h,n_1,k_i,n_2,k_j} &= \mathbb{E}\left[\mathbf{h}_{n_1}(k_i)\mathbf{h}_{n_2}^H(k_j)\right] \\ &= \mathbf{F}_{k_i}\mathbb{E}\left[\bar{\mathbf{h}}_{n_1}\bar{\mathbf{h}}_{n_2}^H\right]\mathbf{F}_{k_j}^H \\ &= \rho^{|n_1-n_2|}\mathbf{F}_{k_i}\left(\mathbf{P}\otimes\mathbf{I}_{N_RN_T}\right)\mathbf{F}_{k_j}^H. \end{aligned} \tag{20}$$

Using the result derived in (20), the closed-form expressions of $\mathbf{R}_{hh}$ and $\mathbf{R}_{\tilde{h}h}$ can be evaluated as below. The auto-correlation matrix $\mathbf{R}_{hh}$ can be derived as

$$\mathbf{R}_{hh} = \mathbf{J}_\rho \otimes \left(\mathbf{F}\tilde{\mathbf{P}}\mathbf{F}^H\right), \tag{21}$$

where we have $\tilde{\mathbf{P}} = (\mathbf{P}\otimes\mathbf{I}_{N_RN_T})$. The matrices $\mathbf{J}_\rho$ and $\mathbf{F}$ are defined as

$$\mathbf{J}_\rho = \begin{bmatrix} 1 & \rho & \dots & \rho^{R-1} \\ \rho & 1 & \dots & \rho^{R-2} \\ \vdots & \vdots & & \vdots \\ \rho^{R-1} & \rho^{R-2} & \dots & 1 \end{bmatrix}, \quad \mathbf{F} = \begin{bmatrix} \mathbf{F}_{k_1} \\ \mathbf{F}_{k_2} \\ \vdots \\ \mathbf{F}_{k_{N_P}} \end{bmatrix}. \tag{22}$$

Similarly, the cross-correlation matrix $\mathbf{R}_{\tilde{h}h}$ can be written as

$$\mathbf{R}_{\tilde{h}h} = \mathbf{J}_\rho \otimes \left(\bar{\mathbf{F}}\tilde{\mathbf{P}}\mathbf{F}^H\right), \tag{23}$$

where the matrix $\bar{\mathbf{F}}$ is defined as

$$\bar{\mathbf{F}} = \begin{bmatrix} \mathbf{F}_1 \\ \mathbf{F}_2 \\ \vdots \\ \mathbf{F}_N \end{bmatrix}. \tag{24}$$

Finally, the 2D-MMSE estimate is obtained as

$$\begin{aligned}\hat{\tilde{\mathbf{h}}} &= \mathbf{R}_{\tilde{h}h}\mathbf{\Phi}^H\left(\mathbf{\Phi}\mathbf{R}_{hh}\mathbf{\Phi}^H + \sigma_w^2\mathbf{I}\right)^{-1}\mathbf{y} \\ &= \left(\mathbf{J}_\rho\otimes\left(\bar{\mathbf{F}}\tilde{\mathbf{P}}\mathbf{F}^H\right)\right)\mathbf{\Phi}^H\left(\mathbf{\Phi}\left(\mathbf{J}_\rho\otimes\left(\mathbf{F}\tilde{\mathbf{P}}\mathbf{F}^H\right)\right)\mathbf{\Phi}^H + \sigma_w^2\mathbf{I}\right)^{-1}\mathbf{y}. \end{aligned} \tag{25}$$

REFERENCES

[1] W. G. Jeon, K. H. Paik, and Y. S. Cho, "Two-dimensional MMSE channel estimation for OFDM systems with transmitter diversity," in *IEEE 54th Vehicular Technology Conference. VTC Fall 2001. Proceedings (Cat. No. 01CH37211)*, vol. 3. IEEE, 2001, pp. 1682–1685.